NSG-3127

COHERENT SUBSTRUCTURE OF TURBULENCE NEAR THE STAGNATION ZONE OF A BLUFF BODY

by

Willy E. Sadeh[1] and Herbert J. Brauer[2]

Colorado State University, Fort Collins, Colorado, USA

Fourth Colloquium on Industrial Aerodynamics

Aachen, Germany

18-20 June 1980

[1]Professor of Engineering and Fluid Mechanics, Department of Civil Engineering.
[2]Research Assistant, ibid.

COHERENT SUBSTRUCTURE OF TURBULENCE NEAR THE STAGNATION ZONE OF A BLUFF BODY

by

Willy Z. Sadeh[1] and Herbert J. Brauer[2]

Colorado State University, Fort Collins, Colorado, USA

ABSTRACT

An experimental investigation of the evolution of freestream turbulence in crossflow about a circular cylinder was conducted in order to identify the existence of a coherent substructure near the stagnation zone of a bluff body. This coherent substructure is the outcome of the amplification of freestream turbulence by the stretching mechanism in diverging flow about a bluff body. Visualization of the flow events clearly revealed the selective stretching of cross-vortex tubes and the emergence of an organized turbulent flow pattern near the cylinder stagnation zone. Significant amplification of the total turbulent energy of the streamwise fluctuating velocity was consistently monitored. Realization of selective amplification at scales larger than the neutral scale of the stagnation flow was indicated by the variation of the discrete streamwise turbulent energy. A most amplified scale, characteristic of the energy-containing eddies within the coherent substructure and commensurate with the boundary-layer thickness, was detected. Penetration of the amplified turbulence into the cylinder boundary layer led to the retardation of separation and to a concurrent decrease in the drag coefficient at subcritical cylinder-diameter Reynolds numbers. The major role played by the amplified turbulence concentrated within the coherent substructure in determining the pressure fluctuations on the upwind face of a bluff body is indicated by the variations of the energy spectra of both incident turbulence and wall pressure fluctuations.

1. INTRODUCTION

The pressure fluctuations on the upwind face of a bluff body in crossflow are primarily caused by the turbulence present in the incident wind. At the same time, the distribution of the mean pressure on the upwind face and along the entire body are markedly affected by the freestream turbulence. These effects of the incident turbulence stem from its selective amplification. Freestream turbulence, no matter how small initially, undergoes significant amplification as it is conveyed by the mean flow toward the bluff body stagnation zone. This turbulence amplification is governed by the stretching of cross-vortex tubes that, in turn, is induced by the flow divergence around a bluff body according to the vorticity-amplification theory [1,2]. The amplification of turbulent energy transpires selectively at scales λ larger than a certain neutral scale λ_0. At scales smaller than the neutral, the turbulence dissipates more rapidly due to the viscous action than it amplifies. The neutral scale λ_0 is determined by each particular flow divergence situation and bluff body geometry.

---

[1]Professor of Engineering and Fluid Mechanics, Department of Civil Engineering.
[2]Research Assistant, ibid.

In order to describe the stretching mechanism and the accompanying turbulence amplification, crossflow about an infinitely long circular cylinder of radius R when the approaching total velocity U_2 contains mainly cross vorticity ω_1 capable of experiencing amplification is examined. This flow situation for a single ideal cross-vortex tube of a scale λ larger than the neutral one initially oriented in the x_1-direction at some station $x_2^{\S}$ upstream of the cylinder stagnation zone along with the system of coordinates used is displayed in Fig. 1. This cross-vortex tube undergoes simultaneous increasing axial stretching and streamwise biased tilting as it is swept by the mean flow toward the stagnation zone of the cylinder as illustrated at several arbitrary streamwise stations x_2', x_2'' and x_2''' in Fig. 1. Its pure axial stretching is governed by the favorable rate of tensile strain $\partial U_1/\partial x_1$ while its streamwise biased tilting is controlled by the appropriate rate of cross strain $\partial U_2/\partial x_1$. Each cross-vortex tube experiences additional axial stretching and acquires a vorticity component ω_2 in the x_2-direction as a result of its streamwise biased tilting. Both the volume and the angular momentum of each cross-vortex tube are conserved throughout its stretching and tilting when viscous dissipation is disregarded. Then its scale λ decreases, its vorticity increases and its accompanying streamwise turbulent velocity u_2 amplifies as depicted in Fig. 1.

The outcome of the stretching and streamwise biased tilting of the cross-vortex tubes is their organization into a coherent substructure near the stagnation zone of a body. This coherent substructure consists ideally of a regular array of standing cross-vortex tubes distributed spanwise and with their cores outside the body boundary layer δ as portrayed in Fig. 2. Within the cells of equal scales of this organized vortex substructure, the rotation alternates in its direction and turbulent energy accumulates. In fact, this coherent substructure represents an array of energy-containing eddies. Most of the turbulence amplification occurs furthermore at a most amplified scale λ_m[3] characteristic of this coherent substructure. This most amplified scale is generally greater than but commensurate with the thickness of the body boundary layer.

A major role in determining the pressure fluctuations and the mean pressure distribution on the forward wall of a bluff body is played by this array of energy-containing eddies and, in particular, by the most amplified scale. They are most effective in the convective transport of momentum (and energy) from the outer flow-i.e., from the flow outside the local forward boundary layer-directly to the wall. Furthermore, penetration of energy-containing eddies into the prevalent body boundary layer affects its nature. They render it turbulent if it was initially laminar and/or they enhance the turbulence within the boundary layer. The wall pressure fluctuations are then determined by the turbulent velocities since they act as a pressure source according to the pressure covariance equation [4,5,6,7].

The wall mean pressure distribution on a bluff body depends upon whether the boundary layer on its forward face is laminar or turbulent. In the case of a regular bluff body, such as a circular cylinder, the penetration of the amplified turbulence into the body boundary layer modifies the wall mean pressure and, particularly, the mean base pressure in a way that retards the separation and even fully forestalls laminar separation. On a bluff body with sharp corners, the separation occurs invariably at the corners independently of the nature of the boundary layer and of the mean pressure distribution on the forward wall. The amplified

turbulence, on the other hand, alters the mean pressure distribution on the upwind face, on the side walls and the base pressure. As a result, the reattachment of the boundary layer along the side walls can be affected by the amplified turbulence. This effect is yet to be investigated.

A brief account of exploratory efforts to identify the amplification of incident turbulence and the realization of a coherent substructure in crossflow about a circular cylinder, to start with, is presented herein.

2. FLOW EVENTS VISUALIZATION

An extensive visual investigation of the turbulent flow patterns near the stagnation zone of a circular cylinder was first undertaken to verify the occurrence there of a coherent substructure. This visualization study was conducted in a 1.83x1.83x27 m (6x6x88 ft) low-speed closed-circuit wind tunnel at Colorado State University using a circular cylinder 16 cm (6-1/4 in) in diameter D and 183 cm (6 ft) long at a cylinder-diameter Reynolds number $Re_D = 8x10^3$ (based on the freestream velocity which was maintained at 0.76 m/s; kinematic viscosity $\nu = 1.5x10^{-5}m^2/s$ $(1.6x10^{-4}ft^2/s)$, air at 20°C (68°F)). A neutral wavelength $\lambda_0 = \pi D/Re_D^{\frac{1}{2}}$ and a laminar boundary layer thickness $\delta = 1.2D/Re_D^{\frac{1}{2}}$ of 5.6 and 2.15 mm, respectively, were expected at this particular Reynolds number [2]. Freestream turbulence was produced in a controlled manner by means of a grid consisting of 24 regularly spaced vertical cylindrical bars (center-to-center interval of 6.35 cm (2-1/2 in), diameter of each rod 1.27 cm (1/2 in)). This grid was installed 116 cm (45-3/4 in) upwind of the cylinder. The vertical orientation of the rods was specifically chosen for generating mainly vorticity susceptible to undergoing amplification by stretching, i.e., vorticity in the x_1-direction (see Fig. 1). Most of the turbulent energy produced by this grid was concentrated at a Strouhal scale of 60.45 mm (2.38 in) (rod Reynolds number 650 to 780, 20% blockage, rod Strouhal number 0.21). This scale was almost 11 times greater than the neutral scale of this stagnation flow. The turbulence intensity (based on local mean velocity) was about 7.7% at the midpoint between the grid and the cylinder. All the details of the experimental setup and procedure are outlined in Ref. 8.

Visualization of the flow in the stream and normal planes (see Fig. 1) was accomplished using titanium dioxide white smoke. Motion pictures of the smoke patterns were shot at a speed of 24 frames/second (41-2/3 ms/frame). Selected movie sequences were analyzed by means of a photo-optical data-analyzer movie projector. Interpretative sketches of single frames were produced by digitizing the pattern of the smoke entrained by a cross-vortex tube. This frame-by-frame examination led to the acquisition of a reasonably quantitative interpretation of the gross flow structure in addition to furnishing an in-depth qualitative perception of the flow pattern. Four representative prints, two for the side view (stream plane) and two for the top view (normal plane), of the frames surveyed along with their corresponding interpretative schematics are displayed in Figs. 3 and 4. The scale, the system of coordinates, the total approaching velocity and the theoretical laminar boundary-layer thickness (a dashed line denoted by letter L) are shown in these sketches.

The entrainment of the smoke filaments by an emerging cross-vortex tube near the stagnation zone is clearly observed in the side-view frames shown in Fig. 3. Occurrence of the stretching is inferable from the distinctly spiral shape of the

cross-vortex tube. The side views permitted the tracing of the time history of a cross-vortex tube from its embryonic stage until its aging phase. In scrutinizing the shape of the cross-vortex tube, it is apparent that its core is outside the laminar boundary layer. The gross scales of the cross-vortex tube, approximated from the interpretative schematics, ranged from 4 to 40 mm (0.16 to 1.60 in). Insofar as the neutral scale was 5.6 mm (0.22 in), vorticity at scales larger than the neutral prevailed near the stagnation zone. This is exactly the cross vorticity that undergoes intensification by stretching which leads, in turn, to the amplification of streamwise turbulence.

An illustration of the coherent vortex substructure near the stagnation zone is provided by the views in the normal plane (top views) given in Fig. 4. Particularly revealing is the persistence of a standing cross-vortex tube whose axis is clearly in the x_1-direction and whose core is outside the boundary layer. A rapid decrease in the scale of the cross-vortex tube across and down its barrel (along its axis in the x_1-direction) is readily perceived. This diminution in the scale is accompanied by an augmentation in the angular velocity owing to the conservation of angular momentum. A gradual increase in the smoke rotational velocity is, in fact, vividly perceivable elsewhere in the motion picture. This continuous scale decrease and the accompanying increase in the rotational velocity attest to the stretching experienced by the cross-vortex tubes. The embayments of the tubular shape, perceived in the second frame shown in Fig. 4, further suggest the presence of two adjacent cross-vortex tubes in which the rotation is in an opposite direction (see Fig. 2). Similar quasi-regular cellular patterns were, as a matter of fact, visualized along the span of the cylinder stagnation zone at many other stations. By and large, the scales of the pathlines in the x_2x_3-plane ranged from 2 to 32 mm (0.08 to 1.26 in) and, thus, they are of same magnitude as their counterparts approximated in the stream plane. Thus, the visualization clearly revealed the existence of a coherent substructure consisting of regularly distributed cross-vortex tubes of roughly the same scale along the span of the cylinder stagnation zone.

3. FREESTREAM TURBULENCE AMPLIFICATION

The evolution of the freestream turbulence as it is conveyed by the diverging mean flow toward the cylinder was surveyed in order to determine its amplification and energy distribution. This investigation was carried out in the same wind tunnel and employing the same turbulence-generating grid as for the visualization study. The survey focused on the measurement of the axial (or streamwise) fluctuating velocity u_2 along the stagnation streamline, i.e., along the x_2-axis (see Fig. 1). This is the sole nonvanishing turbulent velocity component along the stagnation streamline due to symmetry considerations [3]. The measurements were conducted at more than 20 stations between the grid and the cylinder using single-sensor hot-wire anemometers. They were carried out at six subcritical cylinder-diameter Reynolds numbers ranging from 5×10^4 to 2×10^5 and for three different upwind positions of the grid at each Reynolds number. Only a characteristic sample of the results at a cylinder-diameter Reynolds number $Re_D = 1.2\times10^5$-i.e., at a freestream velocity $U_{2\infty} = 11.70$ m/s (38 ft/s)-with the grid installed at an upwind distance $x_{2g} = 7.5D$ (120 cm (47 in)) are reported herein due to space constraints.

The total turbulent energy of the axial fluctuating velocity-i.e., its mean-squared value $\overline{u_2^2}$-is the quantity of interest with regard to the amplification of turbulence. It was computed from the local turbulence intensity and mean velocity data at each station along the x_2-axis. The total streamwise turbulent energy

exhibited a similar general variation in all the cases. To start with, it decayed to some minimum level $\overline{u_{2min}^2}$ with increasing downstream distance from the grid. As the cylinder was approached and the mean flow divergence around it started off, the axial turbulent energy experienced gradual significant amplification up to a certain maximum value due to the stretching mechanism. The peak in the total turbulent energy was consistently found close to the outer edge of the stagnation boundary layer. Inside the latter the total turbulent energy decreased to zero at the cylinder stagnation point since there the fluctuating velocity vanishes. In order to readily determine the relative level of amplification of the total streamwise turbulent energy, it is appropriate to refer it to its minimum value upwind of the cylinder. Then the total dimensionless streamwise turbulent energy is defined by

$$\tilde{\overline{u_2^2}} = \overline{u_2^2}/\overline{u_{2min}^2}, \tag{1}$$

where $\overline{u_{2min}^2}$ is the total minimum turbulent energy between the grid and the cylinder. Essentially, the dimensionless total streamwise turbulent energy represents an amplification ratio. The total minimum turbulent energy and its corresponding turbulence intensity (i.e., $(\overline{u_{2min}^2})^{1/2}/U_{2\infty}$, where $U_{2\infty}$ is the freestream velocity) are viewed as the critical turbulence numbers insofar as the amplification is concerned. It is further necessary to delineate the axial range over which the amplification occurs in terms of a characteristic dimension of the body. To this end, the dimensionless axial distance (see Fig. 1) is expressed by

$$\tilde{x}_2 = x_2/R, \tag{2}$$

in which $R = 8$ cm (3-1/8 in) is the cylinder radius.

A typical distribution of the dimensionless total streamwise turbulent energy (or the amplification ratio) along the stagnation streamline is displayed in Fig. 5. The minimum (or critical) axial turbulent energy $\overline{u_{2min}^2}$, that was about 3533 cm^2/s^2 (3.80 ft^2/s), was monitored at $\tilde{x}_2 = 2.6$. This station was 12.80 cm (5.04 in) upwind of the cylinder which corresponds to a distance of 99.20 cm (39 in) downstream of the grid. At the very same station the critical turbulence intensity, based on the freestream velocity, amounted to only about 5%. The amplification ratio $\tilde{\overline{u_2^2}}$ gradually attained a maximum of about 2.55 over an axial interval extending from $\tilde{x}_2 = 2.6$ to 1.1 (12.80 to 0.80 cm (5.04 to 0.31 in) upwind of the cylinder). This maximum amplification ratio of 255% transpired at a distance of roughly two boundary-layer thicknesses from the cylinder as shown in Fig. 5. The thickness of the actual turbulent stagnation boundary layer, that is marked off onto Fig. 5 by a dashed line designated δ ($\delta = \delta/R$), was about 4 mm (0.16 in), i.e., $\delta = 0.05$. This boundary layer was more than seven times thicker than its initial laminar counterpart whose thickness is about 0.55 mm (0.02 in) at this $Re_D = 1.2 \times 10^5$ ($\delta = 1.2D/Re_D^{1/2}$ [2]). This significant thickening of the boundary layer testifies to the change in its nature from laminar to turbulent owing to the penetration of the amplified turbulent energy into it.

It is further important to point out that the amplification evolved over an axial distance of about 1.5R ($\tilde{x}_2 = 2.6$ to 1.1). This axial length is 15 times larger than the linear deceleration range of the mean velocity that usually extends over a distance of roughly 0.1R upwind of the cylinder [3]. Most of the stretching action is presumably confined within this range according to the vorticity-amplification theory [2]. The results indicate, on the other hand, that

the stretching action extends far beyond the linear velocity deceleration range. Consequently, a higher amplification ratio is reached close to the outer edge of the boundary layer. The large distance within which the stretching occurs further demonstrates that the amplification is not associated with any boundary-layer instability.

A survey of the turbulent energy frequency spectra along the stagnation streamline was next conducted in order to assess the selective amplification of turbulent energy at scales larger than the neutral one. In carrying out this effort, the detection of a most amplified scale λ_m was particularly sought since it is characteristic of the coherent substructure near the cylinder stagnation zone. The amplified turbulent energy concentrated within this coherent substructure is the agent responsible for modifying the nature of the body boundary layer from laminar to turbulent and plays the prime role in determining the wall pressure fluctuations.

The turbulent energy frequency spectra of the axial fluctuating velocity-i.e., $\overline{u_2^2}(n)$, where n is the frequency-were first obtained at each station along the stagnation streamline. A scale λ was next introduced for each frequency n, based on the frozen pattern assumption [9], by means of the relationship

$$\lambda = U_2/n, \tag{3}$$

in which U_2 is the local axial mean velocity. Then the total streamwise turbulent energy at any point (i.e., the mean-square value of the axial fluctuating velocity) is expressed by

$$\overline{u_2^2} = \sum_{i=1}^{\infty} \overline{u_2^2}(\lambda_i), \tag{4}$$

where $\overline{u_2^2}(\lambda_i)$ is the discrete turbulent energy concentrated at any eddy of scale λ_i. The foregoing equation outlines the scale resolution of the turbulent energy spectrum. Consequently, it permits one to examine the change in the discrete streamwise turbulent energy at any desired scale as it is transported toward the cylinder. The discrete turbulent energy at any particular scale λ_i is then derived from the turbulent energy spectra at a succession of points along the stagnation streamline. In order to ascertain the amplification of the discrete streamwise turbulent energy at each scale, it is referred to its level $\overline{u_{20}^2}(\lambda)$ at the station of minimum total turbulent energy. The discrete amplification ratio (or the dimensionless discrete streamwise turbulent energy) at any scale λ is thus expressed by

$$\widetilde{\overline{u_2^2}}(\lambda) = \overline{u_2^2}(\lambda)/\overline{u_{20}^2}(\lambda). \tag{5}$$

A sample of the variations of the dimensionless discrete streamwise turbulent energy at three selected scales larger than the neutral one-viz., at λ = 8, 10 and 20 mm (0.31, 0.39 and 0.79 in) is portrayed in Fig. 6. The discrete turbulent energy at each scale $\overline{u_2^2}(\lambda)$ is referred, according to Eq. (5), to its value $\overline{u_{20}^2}(\lambda)$ monitored at the station of critical total turbulent energy, i.e., to $\overline{u_2^2}(\lambda)$ at $\tilde{x}_2 = 2.6$ (see Fig. 4). At the particular Reynolds number of this flow, (1.2×10^5) the neutral scale of the vorticity-amplification theory $\lambda_0 = 1.45$ mm (0.06 in) ($\lambda_0 = \pi D/Re_D^{\frac{1}{2}}$ [2]). Realization of noticeable amplification of the discrete turbulent energy is clearly discerned at all three scales. The amplification occurred basically over the same interval as that for the total turbulent energy

displayed in Fig. 4. Maximum discrete amplification ratios were reached at all the scales at the outer edge of the actual stagnation boundary layer. The latter, that was about 0.05R thick as previously mentioned, is delineated by dashed line denoted δ in Fig. 6. Inside the boundary layer the discrete turbulent energy gradually decayed to zero at the cylinder stagnation point.

The greatest discrete amplification ratio, that amounted to 73 times, was found at a scale of 8 mm which is 5.52 times larger than the neutral. With increasing scale, the discrete amplification ratio exhibits a continuous decrease. At the other two scales, that are 6.90 and 13.80 times larger than the neutral, discrete amplification ratios of 28 and 23 times, respectively, were monitored. The finding of prime importance is the distinct detection of a most amplified scale λ_m. This scale is representative of the energy-containing eddies within the standing coherent substructure near the cylinder stagnation zone. It is further interesting to point out that this most amplified scale λ_m is commensurate with the thicknesses of both actual turbulent and initial laminar boundary layers. This scale was about twice the thickness of the former (4 mm) and roughly 14 times that of the latter (0.55 mm). One thus can assert that the amplified turbulent energy concentrated within the coherent substructure interacts with the boundary layer and affects its properties. This interaction is responsible for the change in the nature of the boundary layer from laminar to turbulent at the prevailing subcritical Reynolds number.

The modification in the nature of the cylinder boundary layer from laminar to turbulent influences the wall mean pressure distribution and, particularly, the mean base pressure in such a way that the separation is retarded and concurrently the drag coefficient is reduced at the prevailing subcritical Reynolds numbers [10]. At a cylinder-diameter Reynolds number of 1.2×10^5 and same upwind grid position ($x_{2g} = 7.5D$), an increase in the separation angle from its initial laminar value of 80° to about 123° was measured, i.e., a downstream shift in the separation angle of about 43°. Simultaneously, the drag coefficient was reduced by about 28%, i.e., from its original laminar level of 1.04 to 0.748. Similar results were obtained at the other subcritical Reynolds numbers [10]. These results indicate that the penetration of the amplified turbulence into the body boundary layer renders it turbulent, retards the separation and promotes reduction in the drag coefficient despite the prevailing subcritical Reynolds number of the flow.

The agent responsible for the wall pressure fluctuations on the forward face of a bluff body is the turbulence in the incident stream since it acts as a pressure source [4]. Numerous experimental results attest to the strong dependence of the wall pressure fluctuations upon the characteristics of the oncoming turbulence. This dependence is clearly illustrated by the similar variation of the energy spectra of both the incident turbulence and the wall pressure fluctuations on the upwind face of a bluff body with sharp corners reported in Ref. 4 and reproduced in Fig. 7. These energy spectra were obtained with the bluff body in a crossflow at a Reynolds number of about 1.82×10^5 (based on the freestream velocity $U_{2\infty}$ and the front face width) and a characteristic freestream turbulence intensity of about 8%. In Fig. 7, $u_2^2(n)$ and $p^2(n)$ denote the discrete turbulent energy of the streamwise fluctuating velocity and the discrete energy of the wall pressure fluctuations at each frequency n, respectively; while $\overline{u^2}$ and $\overline{p'^2}$ stand for the total turbulent energy of the streamwise turbulent velocity and the total energy of the wall pressure fluctuations, respectively. In addition, a sketch of the bluff body and the system of coordinates is shown in Fig. 7. Both energy spectra reveal a remarkably congruent variation; as the discrete turbulent energy increases so the

discrete energy of the wall pressure fluctuation increases. Moreover, most of both the turbulent energy and the wall pressure fluctuations energy are concentrated within the same frequency range. This behavior of the two energy spectra indicates that the oncoming turbulence emerges at the wall as pressure fluctuations. This energy transfer is effected by the amplified turbulence concentrated within the coherent substructure near the body stagnation zone. The energy-containing eddies of this substructure deliver their energy to the wall pressure fluctuations through the turbulence-turbulence mechanism [4]. Controlling the wall pressure fluctuations on the forward face of a bluff body is consequently a matter of governing the turbulent energy within the coherent substructure through the stretching mechanism.

4. CONCLUDING REMARKS

The evolution of freestream turbulence in crossflow about a circular cylinder was investigated experimentally for the sake of identifying the realization of a coherent substructure near the upwind face of a bluff body. This experimental study consisted of a visualization of the flow events using titanium dioxide white smoke and a detailed hot-wire anemometer survey of the streamwise turbulent velocity. Freestream turbulence was superimposed at scales larger than the neutral using an adequate turbulence-generating grid.

Selective stretching of oncoming cross-vortex tubes and emergence of a coherent substructure near the cylinder stagnation zone were revealed by the flow visualization that was conducted at a Reynolds number of 8×10^3. Occurrence of amplification of the streamwise turbulent energy and of a most amplified scale were indicated by the characteristic results obtained at a Reynolds number of 1.2×10^5. A maximum amplification ratio of the total streamwise turbulent energy of about 255%, relative to its minimum level, was monitored close to the outer edge of the cylinder stagnation boundary layer. Preferred amplification of turbulence at scales larger than the neutral one was demonstrated by the substantial amplification in their discrete turbulent energy. The peak in the discrete turbulent energy was consistently found at all the examined scales at the outer edge of the stagnation boundary layer. A most amplified scale was deduced based on the greatest amplification in the discrete turbulent energy. At this scale, that was roughly 5.52 times the neutral, a maximum amplification of about 73 times was monitored. Much smaller amplifications were recorded at larger scales. The most amplified scale is characteristic of the energy-containing eddies within the coherent substructure. These results demonstrate that the coherent substructure arises from the selective amplification of freestream turbulence that, in turn, is governed by the stretching of cross-vortex tubes in the diverging flow about a bluff body according to the vorticity-amplification theory.

Penetration of the amplified turbulence into the cylinder boundary layer alters its nature from laminar to turbulent at subcritical Reynolds numbers. Retardation of the separation angle by about 43° along with a concomitant reduction in the drag coefficient of 28%, with respect to their laminar counterparts, were obtained. These drastic changes were consequent on the modification of the wall mean pressure distribution caused by the amplified turbulence.

The amplified turbulence is further the prime source for the wall pressure fluctuations on the upwind face of a bluff body. This dependence is clearly revealed by the observed remarkably similar energy spectra of both the oncoming amplified turbulence and the wall pressure fluctuations on the windward face of a bluff body with sharp corners. These results substantiate that the amplified turbulent energy emerges at the wall as pressure fluctuations.

The work reported here is a part of a research program on the structure of turbulence and the effects of incident turbulence upon the boundary layer on bluff bodies and aerodynamic surfaces. Sponsoring of this research program by the NASA Lewis Research Center is gratefully acknowledged. (NSG 3127)

REFERENCES

1. S. P. Sutera, P. F. Maeder and J. Kestin, On the senstivity of heat transfer in the stagnation-point boundary layer to freestream vorticity, J. Fluid Mech., 16 (1963) 497-520.

2. W. Z. Sadeh, S. P. Sutera and P. F. Maeder, Analysis of vorticity amplification in flow approaching a two-dimensional stagnation point, Z. angew. Math. Phys., 21 (1970) 699-716.

3. W. Z. Sadeh, S. P. Sutera and P. F. Maeder, An investigation of vorticity amplification in stagnation flow, Z. angew. Math. Phys., 21 (1970) 717-742.

4. W. Z. Sadeh and J. E. Cermak, Turbulence effect on wall pressure fluctuations, J. Eng. Mech. Div., ASCE, 98 (1972) 1365-1379.

5. B. J. Vickery, Fluctuating lift and drag on a long cylinder of square cross-section in a smooth and in a turbulent stream, J. Fluid Mech., 25 (1966) 481-494.

6. W. W. Willmarth and F. W. Roos, Resolution and structure of the wall pressure field beneath a turbulent boundary layer, J. Fluid Mech., 22 (1965) 81-94.

7. W. W. Willmarth and C. E. Wooldridge, Measurements of the fluctuating pressure at the wall beneath a thick turbulent boundary layer, J. Fluid Mech., 14 (1962) 187-210.

8. W. Z. Sadeh and H. J. Brauer, A visual investigation of turbulence in stagnation flow about a circular cylinder, J. Fluid Mech., in the press.

9. G. I. Taylor, The spectrum of turbulence, Proc. Roy. Soc., A, 164 (1938) 476-490.

10. W. Z. Sadeh, H. J. Brauer and P. P. Sullivan, Freestream turbulence effect on laminar separation on a circular cylinder, Paper No. 79-1476, AIAA 12th Fluid & Plasma Dynamics Conference, Williamsburg, Virginia, 24-26 July 1979.

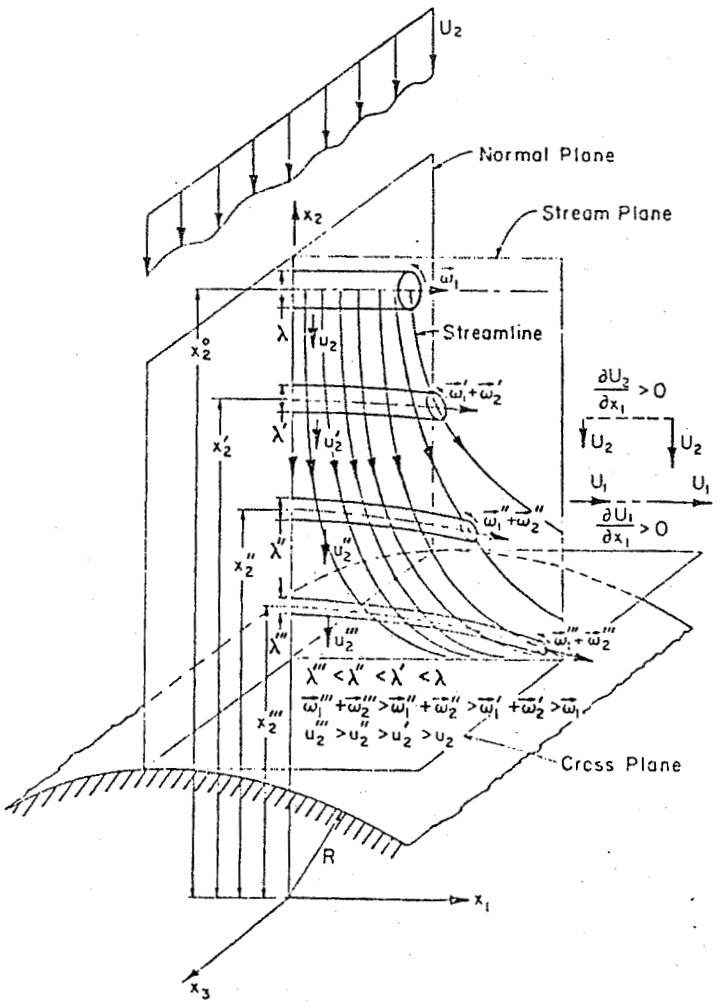

Fig. 1. Stretching and streamwise biased tilting of a cross-vortex tube.

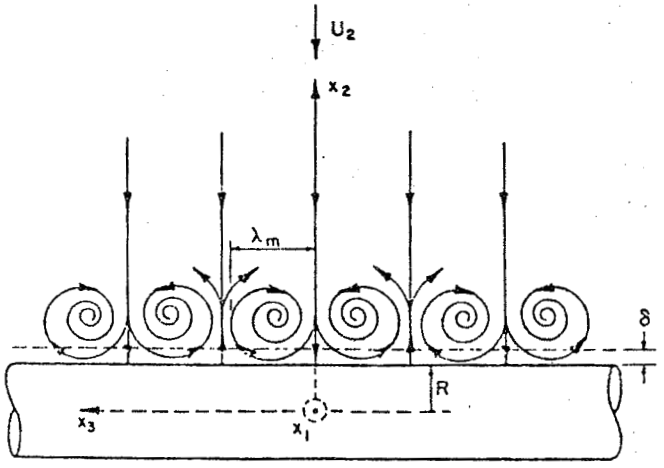

Fig. 2. Coherent substructure of energy-containing eddies near the stagnation zone.

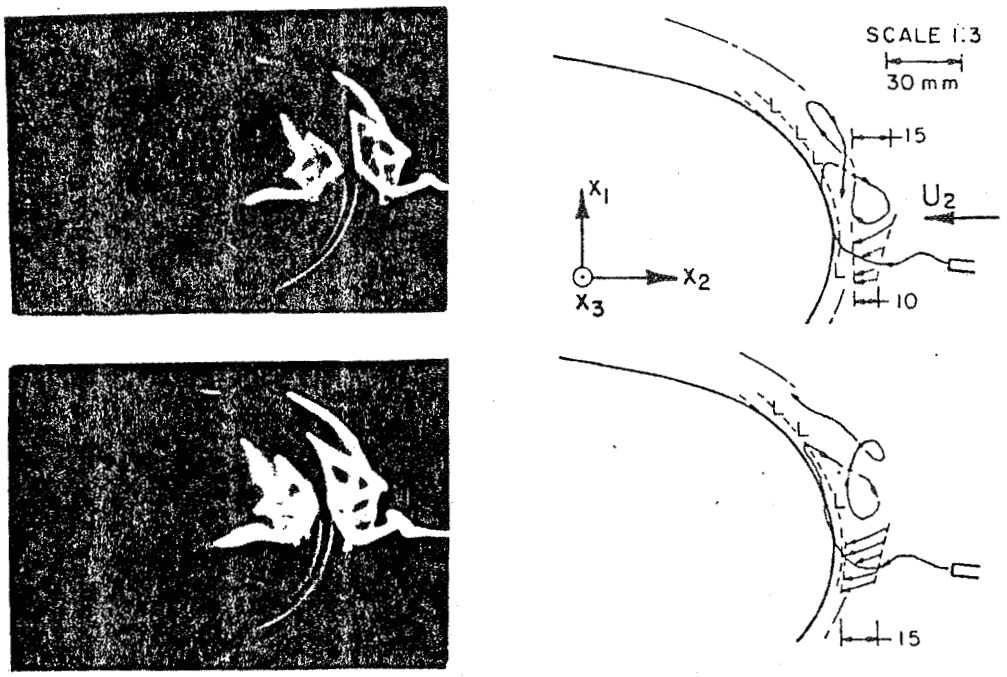

Fig. 3 View of a stretched cross-vortex tube in the stream plane.

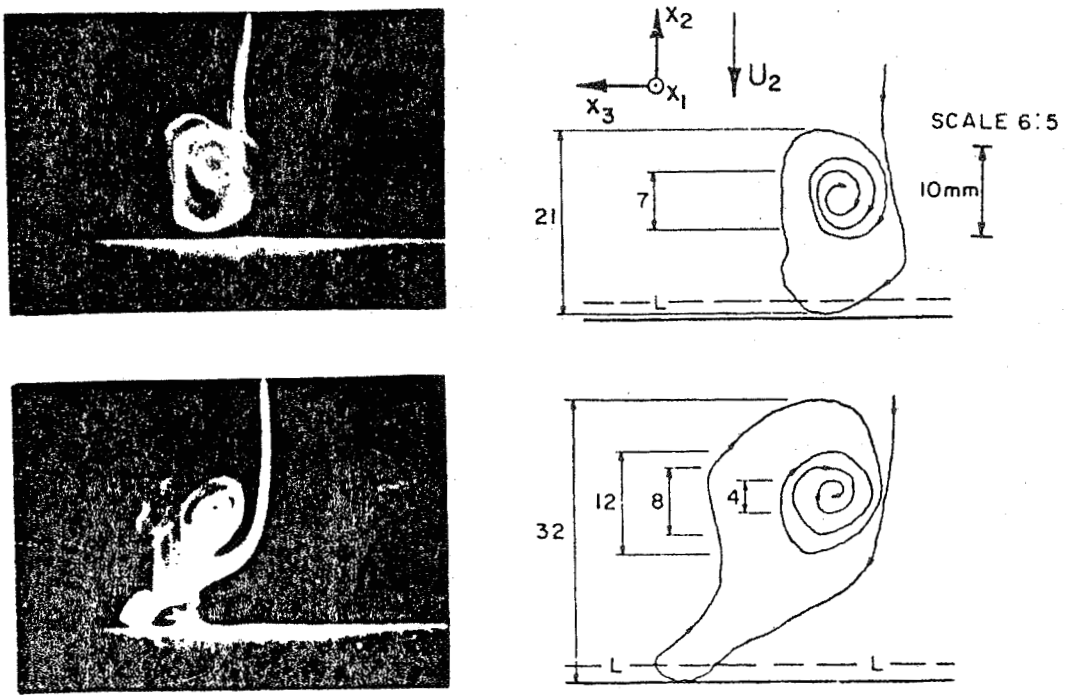

Fig. 4 View of the coherent vortex substructure in the normal plane.

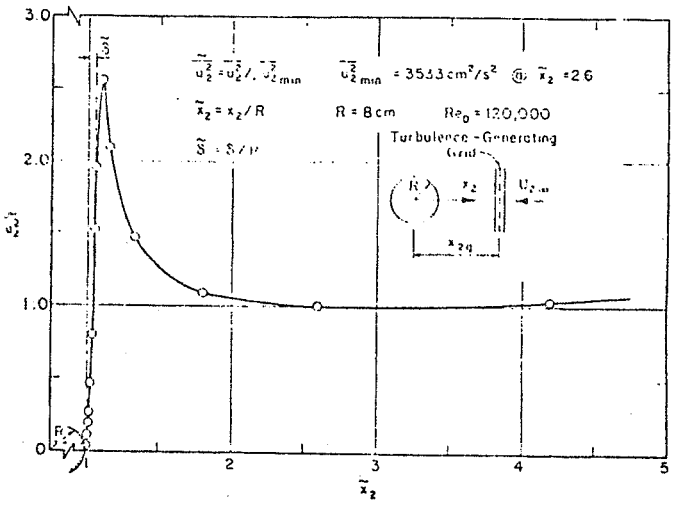

Fig. 5. Amplification ratio of the total streamwise turbulent energy in crossflow about a circular cylinder.

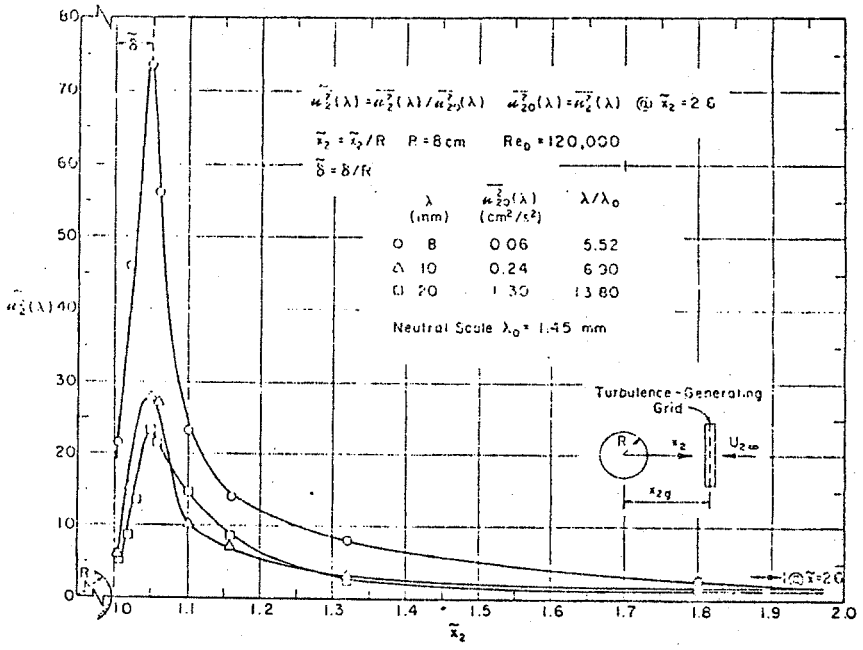

Fig. 6. Amplification of the discrete streamwise turbulent energy at three scales larger than the neutral in crossflow about a circular cylinder.

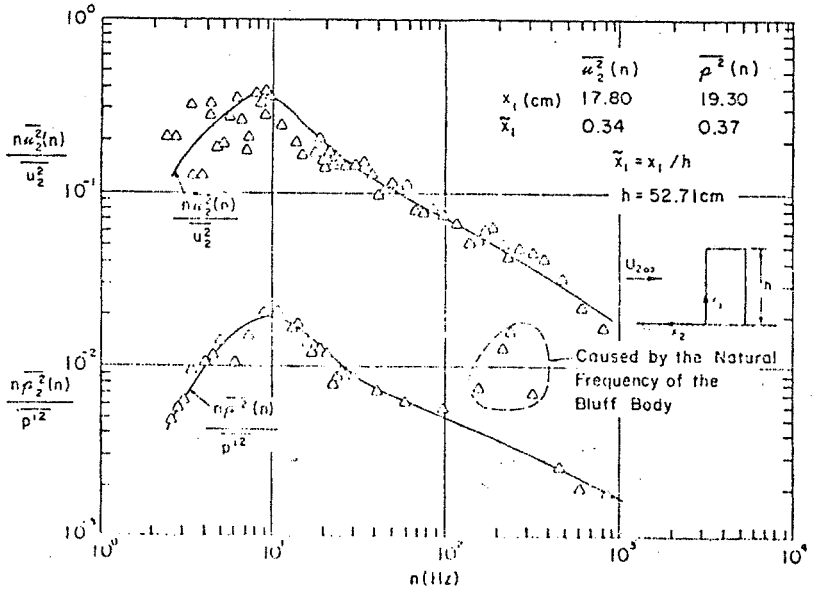

Fig. 7. Energy spectra of incident turbulence and of wall pressure fluctuations on the upwind face of a bluff body with sharp corners.